European Journal of Radiology 84 (2015) 108–116

European Journal of Radiology

journal homepage: www.elsevier.com/locate/ejrad

Predictive value of diffusion-weighted imaging without and with including contrast-enhanced magnetic resonance imaging in image analysis of head and neck squamous cell carcinoma

Daniel P. Noij[a,*], Petra J.W. Pouwels[b,1], Redina Ljumanovic[a,2], Dirk L. Knol[c,3], Patricia Doornaert[d,4], Remco de Bree[e,5], Jonas A. Castelijns[a,2], Pim de Graaf[a,2]

[a] Department of Radiology and Nuclear Medicine, VU University Medical Center, De Boelelaan 1117, Amsterdam, Noord-Holland, The Netherlands
[b] Department of Physics and Medical Technology, VU University Medical Center, De Boelelaan 1117, Amsterdam, Noord-Holland, The Netherlands
[c] Department of Epidemiology and Biostatistics, VU University Medical Center, De Boelelaan 1117, Amsterdam, Noord-Holland, The Netherlands
[d] Department of Radiation Oncology, VU University Medical Center, De Boelelaan 1117, Amsterdam, Noord-Holland, The Netherlands
[e] Department of Otolaryngology – Head and Neck Surgery, VU University Medical Center, De Boelelaan 1117, Amsterdam, Noord-Holland, The Netherlands

ARTICLE INFO

Article history:
Received 22 July 2014
Received in revised form 9 October 2014
Accepted 13 October 2014

Keywords:
Diffusion weighted imaging
Head and neck neoplasms
Magnetic resonance imaging
Observer variation
Prognosis

ABSTRACT

Objectives: To assess disease-free survival (DFS) in head and neck squamous cell carcinoma (HNSCC) treated with (chemo)radiotherapy ([C]RT).
Methods: Pretreatment MR-images of 78 patients were retrospectively studied. Apparent diffusion coefficients (ADC) were calculated with two sets of two *b*-values: 0–750 s/mm^2 (ADC_{750}) and 0–1000 s/mm^2 (ADC_{1000}). One observer assessed tumor volume on T1-WI. Two independent observers assessed ADC-values of primary tumor and largest lymph node in two sessions (i.e. without and with including CE-T1WI in image analysis). Interobserver and intersession agreement were assessed with intraclass correlation coefficients (ICC) separately for ADC_{750} and ADC_{1000}. Lesion volumes and ADC-values were related to DFS using Cox regression analysis.
Results: Median follow-up was 18 months. Interobserver ICC was better without than with CE-T1WI (primary tumor: 0.92 and 0.75–0.83, respectively; lymph node: 0.81–0.83 and 0.61–0.64, respectively). Intersession ICC ranged from 0.84 to 0.89. With CE-T1WI, mean ADC-values of primary tumor and lymph node were higher at both *b*-values than without CE-T1WI ($P < 0.001$). Tumor volume (sensitivity: 73%; specificity: 57%) and lymph node ADC_{1000} (sensitivity: 71–79%; specificity: 77–79%) were independent significant predictors of DFS without and with including CE-T1WI ($P < 0.05$).
Conclusions: Pretreatment primary tumor volume and lymph node ADC_{1000} were significant independent predictors of DFS in HNSCC treated with (C)RT. DFS could be predicted from ADC-values acquired without and with including CE-T1WI in image analysis. The inclusion of CE-T1WI did not result in significant improvements in the predictive value of DWI. DWI without including CE-T1WI was highly reproducible.

1. Introduction

Head and neck cancer accounts for approximately 3% of all malignancies [1]. Treatment selection is based on the best tradeoff between cure rate and quality of life and consists of (a combination) of surgery, chemotherapy and radiotherapy depending on disease stage [2].

With better treatment selection, patients with a high probability of an unfavorable treatment outcome after (chemo)radiotherapy ([C]RT) could undergo primary surgical treatment. The same applies when treatment response to (C)RT can be monitored in an early stage; then (C)RT might be terminated prematurely. After a full (C)RT treatment, salvage surgery with curative intent is still

* Corresponding author. Tel.: +31 20 4442863.
E-mail addresses: d.noij@vumc.nl (D.P. Noij), pjw.pouwels@vumc.nl (P.J.W. Pouwels), rljumanovic@adventh.org (R. Ljumanovic), dirklknol@gmail.com (D.L. Knol), p.doornaert@vumc.nl (P. Doornaert), r.debree@vumc.nl (R. de Bree), j.castelijns@vumc.nl (J.A. Castelijns), p.degraaf@vumc.nl (P. de Graaf).
[1] Tel.: +31 20 4444118.
[2] Tel.: +31 20 4442863.
[3] Tel.: +31 20 444 4474.
[4] Tel.: +31 20 4440414.
[5] Tel.: +31 20 4443689.

http://dx.doi.org/10.1016/j.ejrad.2014.10.015
0720-048X/

possible to perform, however this is not preferred because of a higher risk of complications like impaired wound healing. Moreover, salvage treatment is not always possible because of extension of the residual or recurrent tumor outside its original location. Therefore a minority of patients (21–31%) receives salvage surgery after local failure [3–5].

Diffusion-weighted imaging (DWI) is an emerging magnetic resonance imaging (MRI) technique in response prediction in HNSCC patients treated with (C)RT [6].

DWI is based on differences in water mobility in different tissues which can be quantified into an apparent diffusion coefficient (ADC) [7]. The extent of diffusion weighting depends on the timing and the strength of the gradient and is expressed as a *b*-value. In order to reconstruct an ADC at least two different *b*-values are needed, typically a low (e.g. <150 s/mm^2) and a high *b*-value (e.g. >700 s/mm^2) are used. In hypercellular tissue (e.g. tumor tissue) with a small amount of extracellular space diffusion is restricted, which gives a low ADC-value. In contrary, in hypocellular tissue where diffusion in the extracellular space is facilitated, ADC-values are high. Necrosis and inflammation generally meet these criteria [8,9]. There is still no consensus on the optimal combination of *b*-values, though a combination of $b = 0$ s/mm^2 and $b = 1000$ s/mm^2 is commonly used [9–15].

Diffusion-weighted imaging has shown potential in the prediction of prognosis in patients with head and neck squamous cell carcinoma (HNSCC) treated with (C)RT and to monitor therapy in a very early stage. Higher pretreatment ADC values are associated with adverse prognosis [8,12,13,16]. Furthermore DWI has shown potential to detect central necrosis and (subcentimeter) metastatic lymph nodes [9,15].

Contrast-enhanced imaging is often used to exclude necrosis, which allows that the ADC-value only of the solid part of lesions can be determined [9,15]. To our knowledge there has not been a study that assessed the clinical relevance of using contrast-enhanced imaging for excluding necrosis on DWI. Hatakenaka et al. [10] did suggest that pretreatment ADC would be superior to CE-MRI to predict local failure. Since DWI and contrast-enhanced imaging are based on different properties, both techniques may be synergistic in predicting the outcome of treatment.

The purpose of this study was to assess the prediction of disease-free survival (DFS) and interobserver agreement of DWI without and with including contrast-enhanced T1-weighted imaging (CE-T1WI) in image analysis of HNSCC treated with (C)RT.

2. Methods and materials

2.1. Study population

This retrospective study was approved by the local ethics committee. The requirement for informed consent was waived.

Inclusion criteria were histologically proven HNSCC treated with (C)RT in the oral cavity, oropharynx, hypopharynx or larynx and turbo spin-echo (TSE)-DWI of adequate diagnostic quality for the primary tumor or the lymph node on at least one *b*-value image. Exclusion criteria were previous malignancies in the head and neck area and distant metastases at the start of therapy. All patients were clinically assessed by a head and neck surgeon who performed a physical examination and endoscopic evaluation of the primary tumor. N-stage was assessed using ultrasound-guided fine-needle aspiration cytology. A total of 111 consecutive patients received pre-treatment DWI and (C)RT of the head and neck between August 2009 and December 2011. To allow for optimally comparable data we selected the largest patient group which was scanned on the same MR-system, therefore 18 patients were excluded due to the use of another MR-system. One patient was excluded because no CE-T1WI was acquired. Fourteen patients were excluded because neither the primary tumor nor the largest lymph node was visible on DWI due to small tumor size ($n = 8$) or poor image quality ($n = 4$). Finally, the study consisted of 78 patients. In all 78 patients b1000-imagese were acquired. In 64 of these patients b750-images were also acquired. See Fig. S1 in the Electronic Supplementary Material for a detailed flow-chart of patient inclusion.

Supplementary Fig. S1 related to this article can be found, in the online version, at http://dx.doi.org/10.1016/j.ejrad.2014.10.015.

Radiotherapy was delivered to the primary tumor and affected lymph nodes to a total dose of 70 Gy in 35 fractions of 2 Gy in 70 patients. Three patients received a total dose of 69 Gy in 30 fractions of 2.3 Gy. All these 73 patients received an elective dose to the lymph nodes at risk for microscopic tumor. In 4 patients a total dose of 52 Gy was delivered in 16 fractions of 3.25 Gy. One patient received 60 Gy in 25 fractions of 2.4 Gy. In the these last 5 patients, no elective dose to the lymph node regions was given. Thirty-eight patients received additional chemotherapy (i.e. 100 mg/m^2 cisplatin in the first, fourth and seventh week after the start of radiotherapy ($n = 24$) or 400 mg/m^2 cetuximab one week before the start of radiotherapy followed by 250 mg/m^2 every week during radiotherapy ($n = 14$)). Patient, tumor and treatment characteristics are summarized in Table S1 in the Electronic Supplementary Material. Median time between MRI examinations and the start of treatment was 25 days (range, 7–63 days).

Supplementary Table S1 related to this article can be found, in the online version, at http://dx.doi.org/10.1016/j.ejrad.2014.10.015.

Follow-up consisted of clinical assessment every 6–8 weeks during the first year, every 2–3 months during the second year and every 3–4 months in the third year. Additional imaging and diagnostic procedures were performed in case of clinical suspicion of recurrent disease, residual disease or distant metastases. Positive biopsy or locoregional disease progression within six months after the end of treatment was considered to be residual disease; after six months it was considered to be a locoregional recurrence.

2.2. MR imaging

Imaging was performed on a 1.5 T system (Signa HDxt; GE Healthcare, Milwaukee, WI, United States), using a standard head and neck coil with 29 elements. For all sequences the FOV was 250 mm. DWI was acquired using two PROPELLER sequences with two sets of two *b*-values: $b = 0$ and 750 s/mm^2 and $b = 0$ and 1000 s/mm^2, respectively. ADC-maps were calculated by using two sets of *b*-values: $b = 0$ and 750 s/mm^2 (ADC_{750}) and $b = 0$ and 1000 s/mm^2 (ADC_{1000}). After the administration of 0.4 ml/kg gadoteric acid (Dotarem; Guerbet, Roissy, France) in 72 patients and 0.2 ml/kg gadobutrol (Gadovist; Bayer Schering AG, Berlin, Germany) in 6 patients, CE-T1WI without fat saturation was acquired. An overview of our imaging protocol is provided in Table S2 in the Electronic Supplementary Material.

Supplementary Table S2 related to this article can be found, in the online version, at http://dx.doi.org/10.1016/j.ejrad.2014.10.015.

Because of differences in resolution and to correct for patient movement, CE-T1WI and DWI were co-registered using the linear registration software tool FLIRT from the FSL package (FMRIB Center, Oxford, United Kingdom).

2.3. Image analysis

Images were evaluated with Centricity Radiology RA 600 (version 6.1, GE Healthcare, Milwaukee, WI, USA). Volume of the primary tumor and largest lymph node were assessed on T1-weighted images by one reader (JCA) by drawing manual ROIs

on each slice containing the lesion. The same reader also assessed the short axis diameter of the largest lymph node [17].

Image analysis without and with including CE-T1WI in image analysis was done in two sessions by two radiologists (JCA and PGR) with 21 and 6 years of experience in head and neck radiology. In both sessions observers had access to conventional MR-sequences for anatomical correlation, and patient information regarding age, gender, global tumor location (i.e. oral cavity, oropharynx, larynx and hypopharynx) and TNM-stage, but were blinded to treatment outcome and the results of the other observer. In the first session observers had access to all diffusion sequences (i.e. b0, b750, b1000 and corresponding ADC-maps) but not to the CE-T1WI. Free-hand regions of interest (ROIs) were drawn on the high *b*-value images to delineate the solid parts of the tumor and largest lymph node on the slide that contained the core of the lesion, avoiding areas of necrosis. Solid parts were characterized by a high signal intensity on the high *b*-value images and low signal intensity on the ADC-map. ROIs were copied from the high *b*-value images to the ADC-map. Mean ADC-value and ROI volume were recorded. Image quality of DWI was assessed separately for the primary tumor and largest lymph node using a five-point Likert scale: 1 = inadequate; 2 = moderate; 3 = fair; 4 = good; 5 = excellent.

In the second session observers had access to CE-T1WI weighted images, b0 images and ADC-maps, but not to high *b*-value images. On CE-T1WI single slice free-hand ROIs were placed on the contrast-enhancing part of the tumor and largest lymph node, again areas of necrosis were avoided. The ROI was first copied to the b0-image to verify the anatomical position and subsequently to the ADC-map. Again mean ADC-value and ROI volume were recorded. To minimize recall bias, the second session was at least four weeks after the first. To ensure that the same lesions were assessed in both sessions, observers had access to the slice position of the ROI in the first session.

2.4. Statistical analysis

Statistical analyses were performed using SPSS (version 20.0; Chicago, IL, USA). Wilcoxon signed rank tests were used to compare the image quality of both *b*-values for both observers separately and to compare ROI volumes acquired without and with including CE-T1WI in image analysis. Interobserver agreement and intersession agreement (i.e. between ADC-values acquired without and with including CE-T1WI in image analysis) were assessed by calculating the two-way mixed model intraclass correlation coefficient (ICC) [18]. ICCs can be interpreted according to Nunnally [19]: Techniques with an ICC > 0.80 are reliable for basic research, to be clinically applicable ICCs > 0.90 are necessary.

Mean ADC-values of both observers were used for subsequent analyses. We compared ADC-values derived without and with including CE-T1WI in image analysis by using paired sample *t*-tests and Bland–Altman plots. Paired sample *t*-tests were also used to compare ADC_{750} with ADC_{1000}.

DFS was assessed for various predictors using univariable Cox regression analysis. Significant predictors were tested further with multivariable Cox regression analysis. ROC analyses was performed to determine the optimal cut-off value with the highest Youden Index for lesion volume and ADC-values in predicting DFS. This optimal cut-off was used to create Kaplan–Meier curves of these continuous variables.

3. Results

3.1. Treatment outcome

Median follow-up was 18 months (interquartile rang (IQR), 9–25 months). Five patients were censored because of a second primary tumor. One patient died due to euthanasia. This patient was censored because we did not consider this to be death due to disease progression. Sixty-nine percent (54/78) of the patients remained disease-free during follow-up. During follow-up, biopsies were positive for malignancy in 23% (18/78) of the patients. Five patients had residual disease, eight developed a locoregional recurrence and five patients were diagnosed with distant metastasis.

3.2. Image analysis

In 88% (56/64) of the patients the primary tumor was visible on b750-images, on b1000-images in 79% (62/78). Lymph nodes could be evaluated on b750-images in 96% (49/51) of the patients and b1000-images in 93% (57/61) (Table 1) (Fig. S1).

According to both observers the primary tumor ($P < 0.05$) and largest lymph node ($P > 0.05$) were better depicted on the b750 images than the b1000 images (Table 1). Median primary tumor volume was 7.3 cm^3 (IQR, 2.7–14.6 cm^3) with median lymph node volume being 1.3 cm^3 (IQR, 0.5–4.2 cm^3) and median minimal axial diameter of the largest node being 8.2 mm (IQR, 5.5–15.4 mm). Representative images are shown in Fig. 1.

3.3. Interobserver agreement

Without including CE-T1WI in image analysis ICC for ADC-values of the primary tumor was 0.92 for both *b*-values. For the largest lymph node ICC was 0.75 for the ADC_{750} and 0.83 for the ADC_{1000}. Including CE-T1WI in image analysis resulted in lower ICCs being 0.81 and 0.83 for the primary tumor for the ADC_{750} and ADC_{1000} respectively. In lymph nodes these values were also lower being 0.64 for ADC_{750} and 0.61 for ADC_{1000} (Table 1).

3.4. Comparison between ADC-values and ROI volumes without and with including CE-T1WI in image analysis

Regardless of including CE-T1WI in image analysis ADC_{750} was higher than ADC_{1000} in both primary tumor and lymph node ($P < 0.001$). The Bland–Altman plots are provided in Fig. 2. With inclusion of CE-T1WI, mean ADC-values of primary tumor and lymph node were higher at both *b*-values than without CE-T1WI ($P < 0.001$). Also ROIs were larger when including CE-T1WI. This difference in ROI volume was significant ($P = 0.002$), except for the ADC_{750} of the primary tumor ($P > 0.05$). Biases (i.e. mean difference without and with including CE-T1WI) ranged from -0.14×10^{-3} mm^2/s to -0.18×10^{-3} mm^2/s with ICC ranging from 0.84 to 0.89 (Table 2).

3.5. Survival analysis

Results of ROC analysis are shown in Table 3. Area under the curve ranged from 0.54 to 0.82.

Without including CE-T1WI in image analysis, significant prognostic factors in univariable Cox regression of DFS were large primary tumor volume on T1 ($P = 0.001$), and a high lymph node ADC_{1000} ($P = 0.001$). Primary tumor ADC_{750}, primary tumor ADC_{1000}, lymph node volume on T1, minimal axial diameter on T1 and lymph node ADC_{750} were not significant parameters ($P > 0.05$). Other variables included in univariable Cox regression were: age, gender, treatment, adjuvant treatment, and radiation dose. None of these variables was a significant predictor of DFS ($P > 0.05$). Both significant variables remained significant when adding both primary tumor volume on T1 ($P = 0.009$) and ADC_{1000} of the lymph node ($P = 0.014$) to a multivariable Cox regression model (Table 4).

When including CE-T1WI in image analysis, high lymph node ADC_{1000} ($P < 0.001$) was also a significant predictor of DFS in univariable Cox regression. In a multivariable Cox regression

Table 1
Mean ADC-values, image quality and interobserver agreement for both observers without and with including CE-T1WI in image analysis. Image quality was only assessed in the first session.

Variable	Observer 1			Observer 2			Average		
	ADC (10^{-3} mm^2/s)	Median ROI volume (cm^3)	Image quality	ADC (10^{-3} mm^2/s)	Median ROI volume (cm^3)	Image quality	ADC (10^{-3} mm^2/s)	Median ROI volume (cm^3)	ICC (95%CI)
Without CE-T1WI									
Primary tumor ADC_{750} (n = 56)	1.68 ± 0.29	0.65	3.5*	1.66 ± 0.29	0.65	2.8*	1.67 ± 0.29	0.62	0.92 (0.86–0.95)
Primary tumor ADC_{1000} (n = 62)	1.46 ± 0.26	0.64	3.4	1.47 ± 0.26	0.72	2.7	1.47 ± 0.25	0.68†	0.92 (0.87–0.95)
Lymph node ADC_{750} (n = 49)	1.62 ± 0.25	0.29	3.6	1.62 ± 0.33	0.31	2.8	1.62 ± 0.27	0.29†	0.75 (0.60–0.85)
Lymph node ADC_{1000} (n = 57)	1.43 ± 0.23	0.27	3.5	1.41 ± 0.27	0.31	2.7	1.42 ± 0.24	0.29†	0.83 (0.72–0.89)
With CE-T1WI									
Primary tumor ADC_{750} (n = 56)	1.86 ± 0.35	0.89	–	1.83 ± 0.37	0.67	–	1.85 ± 0.34	0.82	0.81 (0.69–0.82)
Primary tumor ADC_{1000} (n = 62)	1.63 ± 0.29	1.01	–	1.59 ± 0.31	0.69	–	1.61 ± 0.29	0.85	0.83 (0.73–0.89)
Lymph node ADC_{750} (n = 49)	1.75 ± 0.28	0.25	–	1.80 ± 0.37	0.37	–	1.77 ± 0.30	0.30	0.64 (0.42–0.78)
Lymph node ADC_{1000} (n = 57)	1.58 ± 0.28	0.30	–	1.56 ± 0.30	0.42	–	1.57 ± 0.26	0.38	0.61 (0.42–0.75)

Data are expressed as mean ± standard deviation. *Abbreviations*: ADC, apparent diffusion coefficient; CE-T1WI contrast-enhanced T1-weighted imaging; ICC, Intraclass correlation coefficient; ROI, region of interest.

* Significant difference between b-values (P < 0.05).

† Significant difference between ROI volumes without and with CE-T1WI (P = 0.002).

model both primary tumor volume on T1 (P = 0.011) and lymph node ADC_{1000} (P = 0.002) remained significant predictors (Table 4). Kaplan–Meier curves of the significant predictors are shown in Fig. 3.

4. Discussion

To our knowledge this is the first study that assesses the predictive value of DWI without and with including CE-T1WI in image analysis of HNSCC. Hatakenaka et al. [10] suggested that pretreatment ADC would be superior to CE-MRI to predict local failure. We did not find any significant differences in the predictive value of DWI with or without including CE-T1WI in image analysis. The intersession agreement was high (ICC = 0.84–0.89). Differences in ADC-values might be explained by a systematic error due to larger ROI volume when including CE-T1WI in image analysis. This may be caused by peritumoral contrast-enhancement. In both settings high lymph node ADC_{1000} and primary tumor volume were independent significant predictors of DFS. These findings suggest that DWI analysis without CE-T1WI is non-inferior to DWI including CE-T1WI in image analysis for predicting DFSDFS. The inclusion of CE-T1WI did not result in significant improvements in the predictive value of DWI. This suggests that DWI can be used to detect necrosis at a comparable level as CE-T1WI, or at least without clinically significant differences. An advantage of DWI compared to CE-T1WI is that it can be used in patients with renal failure.

In our study high pretreatment lymph node ADC_{1000} was a significant predictor of treatment response. Kim et al. [12] also found high pretreatment ADC of metastatic lymph nodes in HNSCC to be a significant predictor of local failure in a study on 33 patients with a median follow-up of 12 months. Sensitivity and specificity were 65% and 86%, respectively. When the change in ADC-value between pre-treatment DWI and DWI one week after the start of treatment was used, sensitivity increased to 86% and specificity was 83%.

However, in a study on 37 HNSCC patients with a follow-up of at least 2 years performed by King et al. [20], pretreatment ADC was not a significant predictor of local failure. Only ADC changes between DWI examinations before and during treatment showed a significant correlation with treatment outcome. A (large) increase of ADC-values in early follow-up was predictive of local control. Treatment induced cell death may lead to reduced diffusion restriction and therefore a rise in ADC-values. These findings suggest that DWI before and during treatment (e.g. two weeks after the start of (C)RT) provides the highest diagnostic accuracy in response prediction. However, this is not yet implemented in clinical practice because early follow-up MRI findings are not yet incorporated in treatment protocols. Besides there is a logistic challenge, because for reliable repeated ADC measurements patients need to be scanned on the same scanner in the same hospital, ideally in the same position [21].

Malignant tissue is characterized by low ADC value implying high cellularity compared to benign tissue [22]. In order to treat HNSCC with (chemo)radiotherapy high cell turnover (i.e. low ADC) is required as (chemo)radiotherapy mainly targets dividing cells [23,24]. Therefore relatively high pre-treatment ADC may result in adverse prognosis for patients treated with (chemo)radiotherapy [12]. For surgery the relation between ADC and prognosis may be different as more slowly dividing malignancies may be more easy to remove radically, however this is beyond the scope of this article.

It should be noted that abscesses are also characterized by high signal intensity on high b-value imaging combined with a low ADC value and may therefore be difficult to distinguish from malignant tissue. In a study of Koç et al. [25] on patients with necrotic and cystic head and neck lesions abscesses could be differentiated from (necrotic) tumors with a sensitivity and specificity of

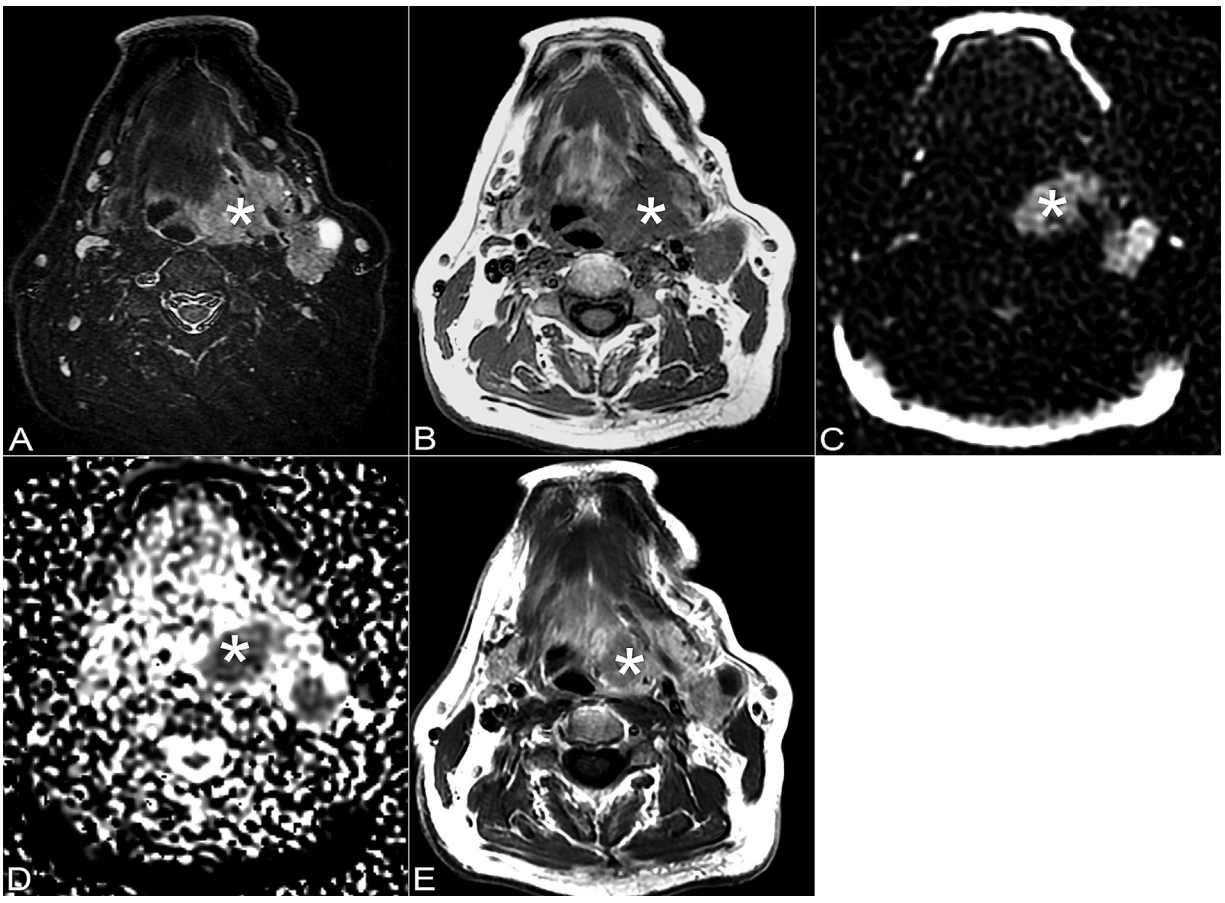

Fig. 1. MR images in a 59-year old male patient with a T3N2c oropharyngeal carcinoma (*). Necrosis (arrow) in the level II lymph node (arrowhead) is detected on (a) STIR (hyperintensity), on (b) T1 minimal hypo-intensity is seen in the necrotic area. The findings of (c) b750 (high signal) and (d) ADC_{750} (high signal) are also indicative of necrosis. On (e) CE-T1WI necrosis is seen due to low contrast-enhancement in the necrotic part of the lymph node (arrow). After 16 months of follow-up this patient remained disease free.

Table 2
Agreement between ADC-values without and with including CE-T1WI in image analysis.

Variable	Bias (10^{-3} mm^2/s)	LoA (10^{-3} mm^2/s)	ICC (95%CI)
Primary tumor ADC_{750}	−0.18	−0.54; 0.18	0.84 (0.74–0.90)
Primary tumor ADC_{1000}	−0.14	−0.42; 0.13	0.88 (0.80–0.92)
Lymph node ADC_{750}	−0.15	−0.42; 0.14	0.89 (0.81–0.94)
Lymph node ADC_{1000}	−0.15	−0.43; 0.12	0.85 (0.75–0.91)

Abbreviations: ADC, Apparent diffusion coefficient; ICC, Intraclass correlation coefficient; LoA, Limits of agreement.

Table 3
Results of ROC-analysis. The highest YI was used to determine the optimal cut-off value.

Parameters	Cut-off	Sensitivity (%)	Specificity (%)	AUC
Tumor volume on T1	7.3 cm^3	73	57	0.66
Lymph node volume on T1	0.8 cm^3	81	40	0.56
Minimal axial diameter	7.6 mm	75	54	0.58
Without CE-T1WI				
Primary tumor ADC_{750}	1.63×10^{-3} mm^2/s	73	53	0.59
Primary tumor ADC_{1000}	1.73×10^{-3} mm^2/s	39	88	0.59
Lymph node ADC_{750}	1.63×10^{-3} mm^2/s	78	60	0.66
Lymph node ADC_{1000}	1.51×10^{-3} mm^2/s	71	74	0.75
With CE-T1WI				
Primary tumor ADC_{750}	1.55×10^{-3} mm^2/s	100	22	0.55
Primary tumor ADC_{1000}	1.44×10^{-3} mm^2/s	85	33	0.54
Lymph node ADC_{750}	1.83×10^{-3} mm^2/s	78	63	0.62
Lymph node ADC_{1000}	1.68×10^{-3} mm^2/s	79	77	0.82

Abbreviations: ADC, apparent diffusion coefficient; AUC, area under the curve; CE-T1WI contrast-enhanced T1-weighted imaging.

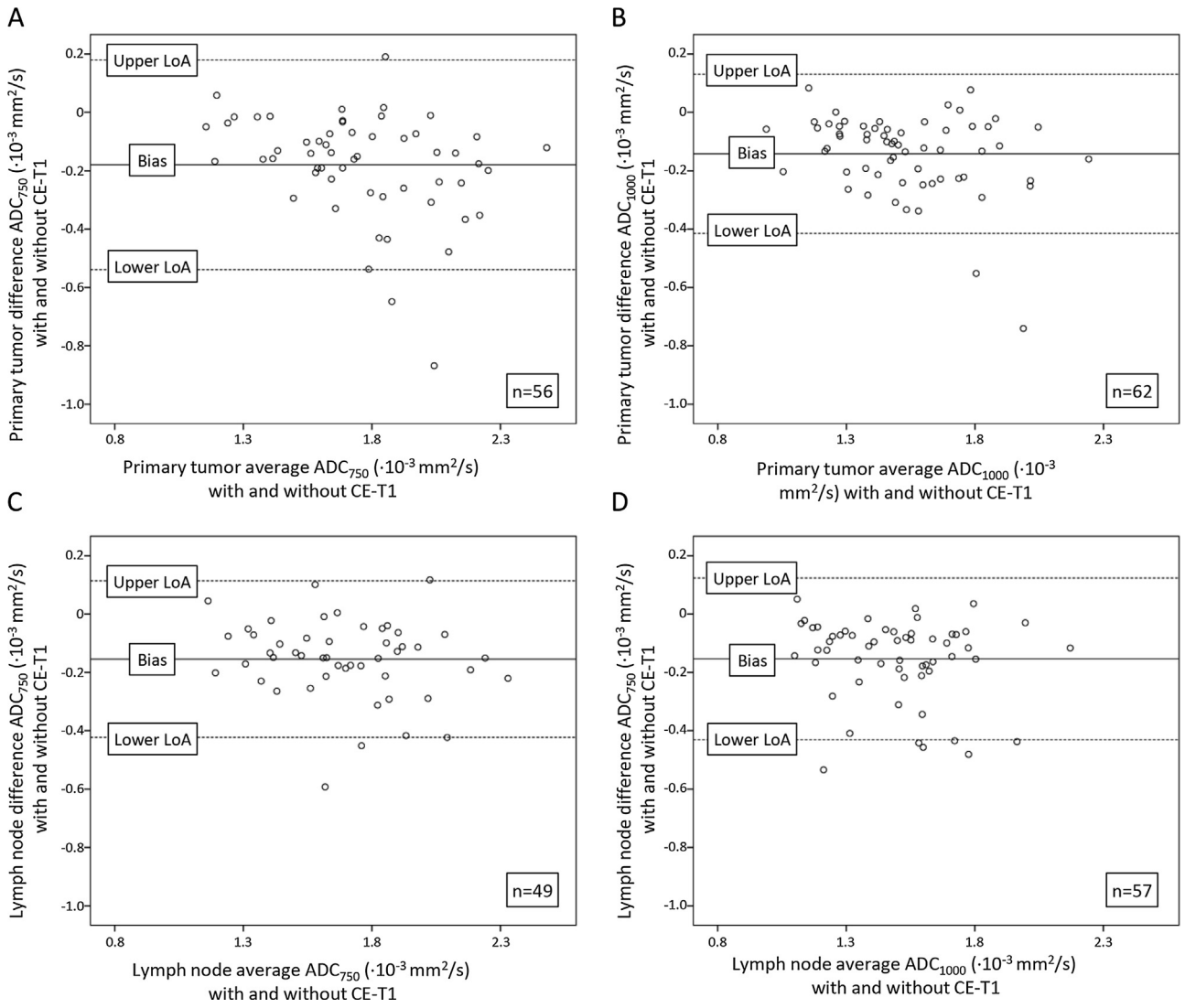

Fig. 2. Bland–Altman plots representing the agreement regarding ADC-measurements without and with including CE-T1WI in image analysis. Positive values indicate a higher ADC-value without including CE-T1WI in image analysis. (a) Primary tumor ADC_{750}, (b) primary tumor ADC_{1000}, (c) lymph node ADC_{750}, (d) lymph node ADC_{1000}.

100%. Abscesses were characterized by even lower ADC values than malignancies. The lower ADC value of abscesses is attributed to the higher cell density in an abscess combined with the presence of proteins and other macromolecules in abscesses [26]. Therefore lesions with high intensity on high *b*-value imaging and low ADC values cannot always considered to be malignant. Other sequences and clinical parameters (e.g. fever and tender lymphadenopathy) may further aid in differentiating abscesses from malignancy.

We used two sets of two *b*-values (0–750 s/mm^2 and 0–1000 s/mm^2). In most clinical studies a maximum *b*-value of 1000 s/mm^2 is used [9–15]. Only King et al. [20] used a maximum *b*-value of 500 s/mm^2 to limit signal loss and image distortion. We used a TSE sequence for DWI instead of the more commonly used echo planar imaging (EPI) sequence. TSE sequences suffer less from geometric distortion, susceptibility artifacts and motion artifacts, but the signal-to-noise-ratio is lower [27]. Therefore the use of a maximum *b*-value of 1000 s/mm^2 could result in a too low signal-to-noise ratio to allow for proper image interpretation. This is supported by our data; the image quality of b750-images was rated slightly higher than b1000-images. Further the primary tumor and lymph node were more frequently visualized on b750-images (88% and 96%, respectively) than on b1000-images (79% and 93%, respectively).

In both primary tumor and lymph node ADC_{750} was higher than ADC_{1000}. This may be explained our assumption of a mono-exponential model. In this model ADC values are lower at higher *b*-values due to perfusion effects at low *b*-values due to a non-linear relation between *b*-values and signal intensity. At higher *b*-values a linear relation exists between *b*-value and signal intensity. ADC values may be better represented with a biexponential model which accounts for the perfusion effects at low *b*-values [28]. It has also been shown that the high *b*-value component (i.e. an ADC value obtained exclusively from *b*-values above 500 s/mm^2) has a stronger correlation with outcome [29].

Verhappen et al. [30] compared primary tumor and lymph node delineation between TSE-DWI and EPI-DWI in twelve patients with HNSCC. They concluded that lesions, in particular small lymph nodes, are more easily visualized with EPI-DWI. This may be explained by a lower signal-to-noise ratio of TSE-DWI compared to EPI-DWI when using a maximum *b*-value of 1000 s/mm^2. However the results of TSE-DWI were more reproducible between observers (ICC = 0.79 for EPI-DWI vs ICC = 0.92 for TSE-DWI). In our study ICC was 0.92 in the primary tumor when only DWI is used. According to the criteria of Nunnally [19] TSE-DWI would be clinically useful only for primary tumor assessment.

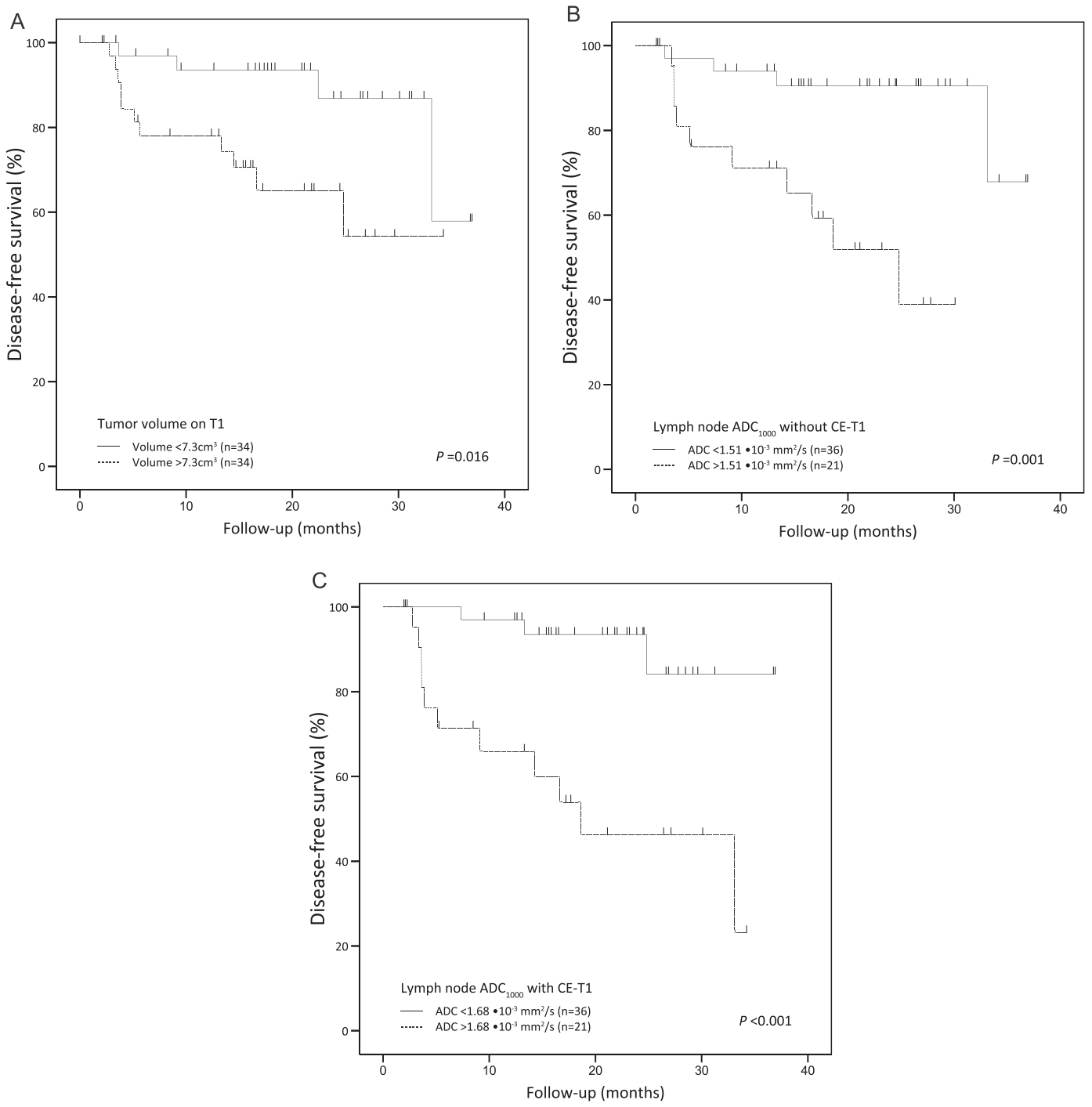

Fig. 3. Kaplan–Meier curves of (A) tumor volume on T1, (B) lymph node ADC_{1000} without including CE-T1WI in image analysis and (C) lymph node ADC_{1000} with including CE-T1WI in image analysis.

In this manuscript we have used mean ADC values per ROI. Standard deviations were also acquired, however these values did not show any significant relations and were therefore not included in the manuscript. Histogram analysis of ADC has been used as marker of tumor heterogeneity (e.g. skewness, kurtosis, ADC_{min} or ADC_{max}) with promising results [31].

This study had some limitations. In the first place, all events in disease-free survival analysis were considered equal, however not all events had the same clinical consequences. We did this because we expect recurrent and residual disease to occur more frequently in the higher tumor stages, regardless of the severity of the event. We also did not assess overall survival, because patients are sometimes referred to other institutions for palliative care. We therefore could not reliably determine the time and cause of death. Secondly, since patients were treated non-surgically it is not fully clear if the largest lymph nodes really contained metastatic tissue. In our institution ultrasound-guided fine-needle aspiration cytology performed by experienced investigators is used for N-staging, which confers the risk of sampling errors. In reviews by de Bree et al. [32] and de Bondt et al. [33] ultrasound guided fine needle aspiration

Table 4
Results of univariable and multivariable Cox regression without and including CE-T1WI in image analysis with the use of CE-T1WI. Significant predictors in univariable Cox regression were tested further with multivariable Cox regression analysis.

Parameter	Univariable Cox regression, *P* value	Multivariable Cox regression, *P* value
Without CE-T1WI		
Primary tumor volume on T1 (cm^3)	0.001	0.009
Primary tumor ADC_{750} (10^{-3} mm^2/s)	0.571	–
Primary tumor ADC_{1000} (10^{-3} mm^2/s)	0.226	–
Lymph node volume on T1	0.763	
Minimal axial lymph node diameter on T1	0.414	
Lymph node ADC_{750} (10^{-3} mm^2/s)	0.202	–
Lymph node ADC_{1000} (10^{-3} mm^2/s)	0.001	0.014
With CE-T1WI		
Primary tumor volume on T1 (cm^3)	0.001	0.011
Primary tumor ADC_{750} (10^{-3} mm^2/s)	0.572	–
Primary tumor ADC_{1000} (10^{-3} mm^2/s)	0.471	–
Lymph node volume on T1	0.763	
Minimal axial lymph node diameter on T1	0.414	
Lymph node ADC_{750} (10^{-3} mm^2/s)	0.240	–
Lymph node ADC_{1000} (10^{-3} mm^2/s)	<0.001	0.002

Abbreviations: ADC, apparent diffusion coefficient; CE-T1WI, contrast-enhanced T1-weighted imaging.

cytology appears to be the best minimally invasive alternative to the gold standard (i.e. histological examination after an elective neck dissection).

Thirdly, 14 patients were excluded because neither tumor nor lymph node was visible at both *b*-values. These patients mainly had small lesions. Observers only had access to global tumor location, but not to the exact tumor location, the outcome of other diagnostic procedures nor patient symptoms, which makes it more difficult to identify small lesions.

5. Conclusions

In conclusion, pretreatment primary tumor volume and the lymph node ADC_{1000} are independent significant predictors of DFS in patients with HNSCC treated with (C)RT. In addition, lymph node ADC_{1000} is a significant predictor with and without including CE-T1WI in image analysis. DWI-analysis without CE-T1WI is highly reproducible, demonstrated by good interobserver agreement. ADC-values were lower without than with including CE-T1W1 in image analsysis. The inclusion of CE-T1WI results in a lower interobserver agreement in measuring ADC on DWI. Therefore pretreatment DWI may be an additional tool to determine patient prognosis. As injection of any contrast agents is not necessary to perform DWI, using DWI without CE-T1WI may result in lower imaging costs with an equal predictive value. Further research is necessary to validate the value of TSE-DWI in response prediction in comparison to EPI-DWI.

Conflict of interest

None.

References

[1] Jemal A, Bray F, Center MM, Ferlay J, Ward E, Forman D. Global cancer statistics. CA: Cancer J Clin 2011;61(2):69–90.
[2] Pignon JP, le Maître A, Maillard E, Bourhis J. Meta-analysis of chemotherapy in head and neck cancer (MACH-NC): an update on 93 randomised trials and 17,346 patients. Radiother Oncol 2009;92(1):4–14.
[3] Kano S, Homma A, Hayashi R, Kawabata K, Yoshino K, Iwae S, et al. Salvage surgery for recurrent oropharyngeal cancer after chemoradiotherapy. Int J Clin Oncol 2013;18(5):817–23.
[4] Röösli C, Studer G, Stoeckli SJ. Salvage treatment for recurrent oropharyngeal squamous cell carcinoma. Head Neck 2010;32(8):989–96.
[5] Zafereo ME, Hanasono MM, Rosenthal DI, Sturgis EM, Lewin JS, Roberts DB, et al. The role of salvage surgery in patients with recurrent squamous cell carcinoma of the oropharynx. Cancer 2009;115(24):5723–33.
[6] Thoeny HC, De Keyzer F, King AD. Diffusion-weighted MR imaging in the head and neck. Radiology 2012;263(1):19–32.
[7] Le Bihan D, Breton E, Lallemand D, Aubin ML, Vignaud J, Laval-Jeantet M. Separation of diffusion and perfusion in intravoxel incoherent motion MR imaging. Radiology 1988;168(2):497–505.
[8] Vandecaveye V, De Keyzer F, Nuyts S, Deraedt K, Dirix P, Hamaekers P, et al. Detection of head and neck squamous cell carcinoma with diffusion weighted MRI after (chemo)radiotherapy: correlation between radiologic and histopathologic findings. Int J Radiat Oncol Biol Phys 2007;67(4):960–71.
[9] Razek AA, Megahed AS, Denewer A, Motamed A, Tawfik A, Nada N. Role of diffusion-weighted magnetic resonance imaging in differentiation between the viable and necrotic parts of head and neck tumors. Acta Radiol 2008;49(3):364–70.
[10] Hatakenaka M, Nakamura K, Yabuuchi H, Shioyama Y, Matsuo Y, Ohnishi K, et al. Pretreatment apparent diffusion coefficient of the primary lesion correlates with local failure in head-and-neck cancer treated with chemoradiotherapy or radiotherapy. Int J Radiat Oncol Biol Phys 2011;81(2):339–45.
[11] Kato H, Kanematsu M, Tanaka O, Mizuta K, Aoki M, Shibata T, et al. Head and neck squamous cell carcinoma: usefulness of diffusion-weighted MR imaging in the prediction of a neoadjuvant therapeutic effect. Eur Radiol 2009;19(1):103–9.
[12] Kim S, Loevner L, Quon H, Sherman E, Weinstein G, Kilger A, et al. Diffusion-weighted magnetic resonance imaging for predicting and detecting early response to chemoradiation therapy of squamous cell carcinomas of the head and neck. Clin Cancer Res 2009;15(3):986–94.
[13] Vandecaveye V, Dirix P, De Keyzer F, de Beeck KO, Vander Poorten V, Roebben I, et al. Predictive value of diffusion-weighted magnetic resonance imaging during chemoradiotherapy for head and neck squamous cell carcinoma. Eur Radiol 2010;20(7):1703–14.
[14] Dirix P, Vandecaveye V, De Keyzer F, Op de Beeck K, Poorten VV, Delaere P, et al. Diffusion-weighted MRI for nodal staging of head and neck squamous cell carcinoma: impact on radiotherapy planning. Int J Radiat Oncol Biol Phys 2010;76(3):761–6.
[15] Vandecaveye V, De Keyzer F, Vander Poorten V, Dirix P, Verbeken E, Nuyts S, et al. Head and neck squamous cell carcinoma: value of diffusion-weighted MR imaging for nodal staging. Radiology 2009;251(1):134–46.
[16] King AD, Mo FK, Yu KH, Yeung DK, Zhou H, Bhatia KS, et al. Squamous cell carcinoma of the head and neck: diffusion-weighted MR imaging for prediction and monitoring of treatment response. Eur Radiol 2010;20(9):2213–20.
[17] Van den Brekel MW, Stel HV, Castelijns JA, Nauta JJ, van der Waal I, Valk J, et al. Cervical lymph node metastasis: assessment of radiologic criteria. Radiology 1990;177(2):379–84.
[18] McGraw KO, Wong SP. Forming inferences about some intraclass correlation coefficients. Psychol Methods 1966;1(1):30–46.
[19] Nunnally JC. Psychometric theory. 1st ed. New York: McGraw Hill; 1967.
[20] King AD, Chow KK, Yu KH, Mo FK, Yeung DK, Yuan J, et al. Head and neck squamous cell carcinoma: diagnostic performance of diffusion-weighted MR imaging for the prediction of treatment response. Radiology 2013;266:531–8.
[21] Sasaki M, Yamada K, Watanabe Y, Matsui M, Ida M, Fujiwara S, et al. Variability in absolute apparent diffusion coefficient values across different platforms may be substantial: a multivendor, multi-institutional comparison study. Radiology 2008;249(2):624–30.
[22] Gupta RK, Cloughesy TF, Sinha U, Garakian J, Lazareff J, Rubino G, et al. Relationships between choline magnetic resonance spectroscopy, apparent diffusion coefficient and quantitative histopathology in human glioma. J Neurooncol 2000;50(3):215–26.
[23] Marcu LG, Bezak E. Neoadjuvant cisplatin for head and neck cancer: simulation of a novel schedule for improved therapeutic ratio. J Theor Biol 2012;297:41–7, http://dx.doi.org/10.1016/j.jtbi.2011.12.001.
[24] Pawlik TM, Keyomarsi K. Role of cell cycle in mediating sensitivity to radiotherapy. Int J Radiat Oncol Biol Phys 2004;59(4):928–42.
[25] Koç O, Paksoy Y, Erayman I, Kivrak AS, Arbag H. Role of diffusion weighted MR in the discrimination diagnosis of the cystic and/or necrotic head and neck lesions. Eur J Radiol 2007;62(2):205–13.
[26] Mishra AM, Gupta RK, Saksena S, Prasad KN, Pandey CM, Rathore D, et al. Biological correlates of diffusivity in brain abscess. Magn Reson Med 2005;54(4):878–85.
[27] Pipe JG, Farthing VG, Forbes KP. Multishot diffusion-weighted FSE using PROPELLER MRI. Magn Reson Med 2002;47(1):42–52.
[28] Chandarana H, Lee VS, Hecht E, Taouli B, Sigmund EE. Comparison of biexponential and monoexponential model of diffusion weighted imaging in evaluation of renal lesions: preliminary experience. Investig Radiol 2011;46(5):285–91, http://dx.doi.org/10.1097/RLI.0b013e3181ffc485.
[29] Lambrecht M, Van Calster B, Vandecaveye V, De Keyzer F, Roebben I, Hermans R. Integrating pretreatment diffusion weighted MRI into a multivariable prognostic model for head and neck squamous cell carcinoma. Radiother Oncol 2014;110(3):429–34, http://dx.doi.org/10.1016/j.radonc.2014.01.004.

[30] Verhappen MH, Pouwels PJ, Ljumanovic R, van der Putten L, Knol DL, De Bree R, et al. Diffusion-weighted MR imaging in head and neck cancer: comparison between half-Fourier acquired single-shot turbo spin-echo and EPI techniques. Am J Neuroradiol 2012;33(7):1239–46.

[31] Ahn SJ, Choi SH, Kim YJ, Kim KG, Sohn CH, Han MH, et al. Histogram analysis of apparent diffusion coefficient map of standard and high *B*-value diffusion MR imaging in head and neck squamous cell carcinoma: a correlation study with histological grade. Acad Radiol 2012;19(10):1233–40, http://dx.doi.org/10.1016/j.acra.2012.04.019.

[32] Bree RD, Takes RP, Castelijns JA, Medina JE, Stoeckli SJ, Mancuso AA, et al. Advances in diagnostic modalities to detect occult lymph node metastases in head and neck squamous cell carcinoma. Head Neck 2014, http://dx.doi.org/10.1002/hed.23814.

[33] de Bondt RB, Nelemans PJ, Hofman PA, Casselman JW, Kremer B, van Engelshoven JM, et al. Detection of lymph node metastases in head and neck cancer: a meta-analysis comparing US, USgFNAC, CT and MR imaging. Eur J Radiol 2007;64(2):266–72.